Marquette University
e-Publications@Marquette

Civil and Environmental Engineering Faculty Research and Publications

Civil and Environmental Engineering, Department of

Framework for Event-based Semidistributed Modeling that Unifies the SCS-CN Method, VIC, PDM, and TOPMODEL

Mark Bartlett
Duke University

Anthony J. Parolari
Marquette University, anthony.parolari@marquette.edu

Jeffrey McDonnell
University of Saskatchewan

Amilcare Porporato
Duke University

Framework for event-based semidistributed modeling that unifies the SCS-CN method, VIC, PDM, and TOPMODEL

M. S. Bartlett[1], A. J. Parolari[1], J. J. McDonnell[2,3], and A. Porporato[1]

[1]Department of Civil and Environmental Engineering, Duke University, Durham, North Carolina, USA, [2]Global Institute for Water Security, University of Saskatchewan, Saskatoon, Saskatchewan, Canada, [3]School of Geosciences, University of Aberdeen, Aberdeen, UK

Abstract Hydrologists and engineers may choose from a range of semidistributed rainfall-runoff models such as VIC, PDM, and TOPMODEL, all of which predict runoff from a distribution of watershed properties. However, these models are not easily compared to event-based data and are missing ready-to-use analytical expressions that are analogous to the SCS-CN method. The SCS-CN method is an event-based model that describes the runoff response with a rainfall-runoff curve that is a function of the cumulative storm rainfall and antecedent wetness condition. Here we develop an event-based probabilistic storage framework and distill semidistributed models into analytical, event-based expressions for describing the rainfall-runoff response. The event-based versions called VICx, PDMx, and TOPMODELx also are extended with a spatial description of the runoff concept of "prethreshold" and "threshold-excess" runoff, which occur, respectively, before and after infiltration exceeds a storage capacity threshold. For total storm rainfall and antecedent wetness conditions, the resulting ready-to-use analytical expressions define the source areas (fraction of the watershed) that produce runoff by each mechanism. They also define the probability density function (PDF) representing the spatial variability of runoff depths that are cumulative values for the storm duration, and the average unit area runoff, which describes the so-called runoff curve. These new event-based semidistributed models and the traditional SCS-CN method are unified by the same general expression for the runoff curve. Since the general runoff curve may incorporate different model distributions, it may ease the way for relating such distributions to land use, climate, topography, ecology, geology, and other characteristics.

1. Introduction

Ideally, a mathematical framework for rainfall-runoff modeling should be applicable to watersheds everywhere. Runoff at a point is classified as one of three physical processes, i.e., infiltration excess overland flow, saturation excess overland flow, and subsurface storm flow, all of which may be considered as a similar threshold-initiated process once different watershed conditions are taken into account [*McDonnell*, 2013; *Dunne*, 1983]. The runoff process is controlled by topographic conditions, as well as geological and ecological controls. By mapping runoff processes to the spatially heterogeneous values of ecological and geological properties, a model should predict runoff according to the prevailing climate and local topographic conditions. Following this notion, *Freeze and Harlan* [1969] outlined the "fully distributed" modeling approach where small-scale physics including runoff processes are explicitly mapped to watershed heterogeneities that are spatially resolved to the grid cell elements subdividing the watershed model.

However, fully distributed models typically have significant data requirements for calibration [*Semenova and Beven*, 2015; *McDonnell et al.*, 2007]. As a result, hydrologists often use simpler spatially lumped models such as the event-based Soil Conservation Service (now the Natural Resources Conservation Service) Curve Number (SCS-CN) method and semidistributed rainfall-runoff models [e.g., *Ponce and Hawkins*, 1996; *Beven*, 2012]. Semidistributed models typically operate in continuous time (discretized into time steps), and in lieu of the variability of the grid cells of fully distributed models, they use a distribution, which is typically of water storage capacity. For the distribution of water storage capacity, the semidistributed Variable Infiltration Capacity (VIC) model [*Wood et al.*, 1992; *Liang et al.*, 1994] and probability distributed model (PDM) [*Moore*, 1985] assume a versatile probability density function (PDF). Alternatively, the semidistributed TOP-MODEL (TOPography-based hydrologic MODEL) defines similar watershed points according to the

topographic index [*Beven and Kirkby*, 1979]. However, this topographic index acts as the basis for the distribution of storage capacity values [*Sivapalan et al.*, 1997].

Previous studies have explored different water storage capacity distributions [*Moore and Clarke*, 1981], examined the physical basis of semidistributed model assumptions [*Franchini et al.*, 1996], compared semidistributed modeling approaches [e.g., *Habets and Saulnier*, 2001; *Warrach et al.*, 2002], analyzed the effects from spatially variable precipitation [*Sivapalan et al.*, 1997; *Liang et al.*, 1996], and exploited combinations of different semidistributed assumptions [e.g., *Noto*, 2013]. In general, most semidistributed models assume the same functional form for direct runoff, as the product of the rainfall rate and the threshold-saturated area [*Kavetski et al.*, 2003]. Recent modeling frameworks, e.g., Framework for Understanding Structural Errors (FUSE) [*Clark et al.*, 2008] and SUPERFLEX [*Fenicia et al.*, 2011], use these equivalent functional forms interchangeably, recognizing that certain model structures may be best suited for certain watershed characteristics. While components of semidistributed models (such as a saturated variable source area (VSA)) have been incorporated with event-based models such as the SCS-CN method [e.g., *Chen and Wu*, 2012], semidistributed models have yet to be given an event-based representation where the cumulative storm runoff is a function of the cumulative storm rainfall and antecedent wetness conditions.

Here we pose a suite of semidistributed models in event-based form by following the *Bartlett et al.* [2016] ProStor framework where the rainfall-runoff response at a point is upscaled to a watershed scale based on a probabilistic joint distribution of storage capacity thresholds and the antecedent soil moisture status. Following the framework, each semidistributed model can be distilled to a basic set of analytical expressions for describing the event-based rainfall-runoff response. When given the total storm rainfall and antecedent watershed wetness status, these expressions define, the source areas (fraction of watershed) that produce runoff by a specific mechanism, the probability density function (PDF) that describes the spatial distribution of runoff, and the (unit area) average runoff. The expression for average runoff, commonly called a runoff curve [e.g., *Descheemaeker et al.*, 2006; *Wine et al.*, 2012], accounts for the spatial variability of rainfall and water storage. Notably, for exponentially distributed rainfall over the watershed, the semidistributed models and the SCS-CN method are unified by the same canonical form of the runoff curve (e.g., equation (10)).

In developing each event-based model, we assume the same point rainfall-runoff response that extended the SCS-CN method to the SCS-CNx method [*Bartlett et al.*, 2016]. This response consists of a fraction of area where runoff occurs both before and after infiltration exceeds the storage capacity threshold, and a complementary area where runoff only occurs episodically when infiltration exceeds the storage capacity threshold. This area represents the original runoff response formulation of VIC, PDM, and TOPMODEL. In comparison, the new event-based model forms (called VICx, PDMx, and TOPMODELx) are extended with the additional "pre-threshold" runoff response that occurs before infiltration exceeds the storage capacity threshold.

2. Extended Event-Based Models

The fundamental underlying concept of semidistributed modeling is that the distribution of watershed heterogeneity is the basis for a water storage capacity distribution represented with a probability density function (PDF). These water storage capacity PDFs are the basis for deriving the corresponding event-based models.

2.1. ProStor Framework for Event-Based Rainfall-Runoff Response

A semidistributed model may be described by a joint distribution of the soil moisture deficit, c, and water storage capacity, w, which describe the potential retention $S = cw$ [see *Bartlett et al.*, 2016]. In an event-based representation, c and S are considered antecedent values immediately prior to the start of the storm, while the point values of rainfall, R, and runoff, Q, represent cumulative depths for the storm duration [see *Bartlett et al.*, 2016, Figure 1]. The spatial variability of these values may be described by the probabilistic storage (ProStor) framework of the joint PDF

$$p_{QRcw}(Q, R, c, w) = p_{Q|Rcw}(Q|R, c, w)p_R(R)p_{cw}(c, w), \tag{1}$$

where $p_{Q|Rcw}(Q|R, c, w)$ is the runoff PDF conditional on R, c, and w; $p_R(R)$ is the PDF of rainfall; and $p_{cw}(c, w)$ is the joint PDF of the antecedent soil moisture deficit and storage capacity. As indicated by these PDFs, rainfall, R, is reasonably assumed to be statistically independent of both the antecedent soil moisture deficit, c, and storage capacity, w [e.g., *Rodríguez-Iturbe and Porporato*, 2004].
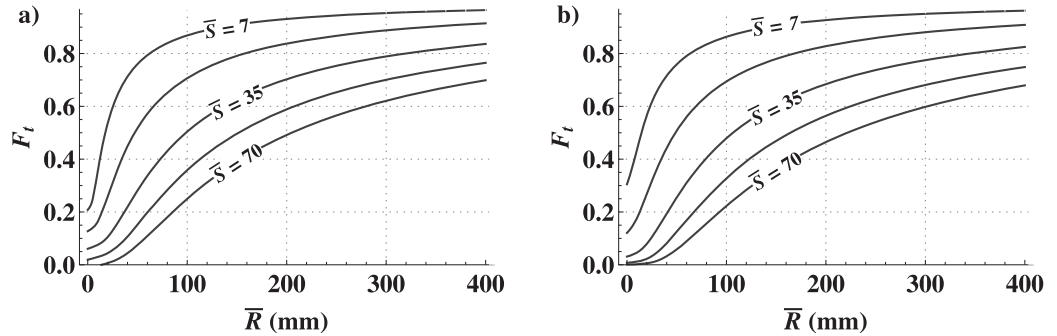
Figure 1. The fraction area with threshold-excess runoff for different watershed average antecedent potential retentions, $\bar{S}$, for (a) VICx/PDMx and (b) TOPMODELx. See Table 3 for parameter values.

If runoff at a watershed point is modeled as a deterministic function, i.e.,

$$Q = Q(R, c, w), \tag{2}$$

then the joint PDF becomes

$$p_{Q|Rcw}(Q|R, c, w) = \delta(Q(R, c, w) - Q)p_R(R)p_{cw}(c, w), \tag{3}$$

where the conditional distribution $p_{Q|Rcw}(Q|R, c, w)$ is now represented by the point mass of probability $\delta(Q(R, c, w) - Q)$, for which $\delta(\cdot)$ is the Dirac delta function. The PDF describing the spatial distribution of runoff is found by integrating equation (3) over the remaining variables (i.e., R, c, and w), while the lumped (unit area) runoff response (i.e., the runoff curve) is the average of equation (3) [*Bartlett et al.*, 2016]. Framework variables and parameters are listed in Table 1.

2.2. The Joint PDF of Antecedent Soil Moisture and Storage Capacity

For the semidistributed models of VIC, PDM, and TOPMODEL, it is possible to show that the joint PDF $p_{cw}(c, w)$ is approximated with a form that is explicitly dependent on the spatial average $\bar{S}$, i.e.,

$$\hat{p}_{cw}(c, w; \bar{S}) = \begin{cases} \delta(cw)p_w(w) & \text{for} \quad 0 \leq w < P_w^{-1}[F(\bar{S})] \\ \\ \delta(cw - w + P_w^{-1}[F(\bar{S})])p_w(w) & P_w^{-1}[F(\bar{S})] \leq w < w_{\max} \end{cases}, \tag{4}$$

where $P_w^{-1}[\cdot]$ is the quantile function of the respective model (Table 2), and $P_w^{-1}[F(\bar{S})]$ represents the water storage capacity, w, at the edge of the prestorm area of threshold saturation, $F(\bar{S})$. Note that the conditional PDF $p_{c|w}(c|w)$, which is represented by $\hat{p}_{c|w}(c|w; \bar{S})$, consists of the point masses of probability $\delta(cw)$ and $\delta(cw - w + P_w^{-1}[F(\bar{S})])$ that, respectively, indicate $cw = 0$ and $cw = w - P_w^{-1}[F(\bar{S})]$ with probability 1.

The fraction of preexisting threshold-saturated area, $F(\bar{S})$, is found from the self-consistent condition [*Bartlett et al.*, 2016]

$$\bar{S} = \int_0^{K(\bar{S})} \int_{P_w^{-1}[F(\bar{S})]}^{w_{\max}} S\delta(S - w + P_w^{-1}[F(\bar{S})])p_w(w)dwdS, \tag{5}$$

where $K(\bar{S}) = w_{\max} - P_w^{-1}[F(\bar{S})]$, and the integrand is the second term of the r.h.s of equation (4) transformed by a change of variables for $S = cw$ [*Bendat and Piersol*, 2011] and modified according to the scaling property of the delta function. The delta function of equation (5) is evaluated using the property presented in *Au and Tam*

Table 1. ProStor Variables and Parameters[a]

Symbol	Description
R	Storm event rainfall depth at a point [L]
w	Water storage capacity depth at a point [L]
c	Antecedent soil moisture deficit at a point, $(1-x)$
x	Antecedent soil moisture at a point, $(1-c)$
S	Antecedent potential retention at a point, $S = cw$ [L]
F_t	Fraction of watershed with threshold-excess runoff
Q	Storm event runoff depth at a point [L]
Q_p	Prethreshold runoff depth at a point over $(1-F_t)$
Q_t	Threshold-excess runoff depth at a point over F_t
β	Fraction of watershed with non-zero prethreshold runoff
P_l	Prethreshold runoff index, $P_l = \beta(1-\bar{c})$
ξ	Shape parameter of the storage capacity PDF $p_w(w)$

[a]Variables in the text with an overline bar indicate a spatial average (unit area) depth value, e.g., for the point rainfall depth, R, the average (unit area) value is denoted by $\bar{R}$. All values have dimensions of length except c, x, β, P_l, ξ, and F_t, which are dimensionless.

Table 2. VIC/PDM and TOPMODEL Expressions

Expression	VIC/PDM	TOPMODEL
Storage capacity dist.	Pareto	Mirrored Exponential[b]
Storage capacity PDF[a]	$p_w(w) = \dfrac{\left(\frac{w_{\max}-w}{w_{\max}}\right)^{1/\xi}}{(w_{\max}-w)\xi}$	$p_w(w) = C_1 \dfrac{\xi}{w_{\max}} e^{-\frac{\xi}{w_{\max}}(w_{\max}-w)}$
Inverse CDF (quantile function)	$P_w^{-1}(F) = w_{\max} - w_{\max}(1-F)^{\xi}$	$P_w^{-1}(F) = \dfrac{w_{\max}}{\xi}\ln\left(1+F(e^{\xi}-1)\right)$
Avg. storage capacity	$\bar{w} = \dfrac{w_{\max}\,\xi}{1+\xi}$	$\bar{w} = w_{\max}\left(C_1 - \dfrac{1}{\xi}\right)$
Avg. potential retention	$\bar{S} = \bar{w}(1-F)^{\xi+1}$	$\bar{S} = \dfrac{\bar{w}}{C_1\xi-1}\left(F - C_1\ln\left(\dfrac{Fe^{\xi}}{C_1}+1\right)\right) + \bar{w}$
Antecedent sat. area[c]	$F(\bar{S}) = 1 - \left(\dfrac{\bar{S}}{\bar{w}}\right)^{1/(1+\xi)}$	$F(\bar{S}) = 1 - C_1 - C_1 W\left(-e^{-\left(1+\frac{\bar{S}(C_1\xi-1)}{\bar{w}C_1}\right)}\right)$
Avg. soil moisture deficit[d]	$\bar{c} = (1-F(\bar{S}))$ $\cdot\left(1 - {}_2F_1\left(1,1;1+\frac{1}{\xi};1+\frac{1}{(1-F(\bar{S}))^{\xi}-1}\right)\right)$	$\bar{c} = 1 - F(\bar{S})$ $+ C_1 e^{-\xi}\ln\left(\dfrac{F(\bar{S})e^{\xi}}{C_1}+1\right)\left(\text{li}\left(\dfrac{F(\bar{S})e^{\xi}}{C_1}+1\right) - \text{Ei}(\xi)\right)$

[a]For values of $0 < w < w_{\max}$ and ξ is the shape parameter of the respective PDF. In the case of TOPMODEL, $\xi = \frac{\kappa_{\max}-\kappa_{\min}}{\kappa_s}$ and $C_1 = \frac{1}{1-e^{-\xi}}$ (Appendix B).
[b]Derived from a truncated exponential PDF representation of the topographic index distribution (Appendix B).
[c]Where $W(\cdot)$ is the Lambert W-function [*Olver et al.*, 2010, p. 111] given in Matlab by lambertw($\cdot$) and in Mathematica by ProductLog($\cdot$). Note that Excel requires an add-in to calculate the Lambert function.
[d]Where ${}_2F_1(\cdot,\cdot;\cdot;\cdot)$ is the hypergeometric function [*Olver et al.*, 2010, p. 384] given in Matlab by ${}_2F_1(a,b;c;d) =$ hypergeom([a, b], c, d) and in Mathematica by ${}_2F_1(a,b;c;d) =$ Hypergeometric2F1[a, b, c, d]. li($\cdot$) and Ei($\cdot$) are the respective exponential and log integrals [*Olver et al.*, 2010, p. 150].

[1999]. For each assumed storage capacity PDF $p_w(w)$, equation (5) is solved for the functional form of $F(\bar{S})$ (see Table 2). Note that the $F(\bar{S})$ for VIC/PDM (Table 2) was previously found by *Kavetski et al.* [2003] by integrating the quantile function of Table 2 based on assumptions for the conditional soil moisture distribution, which are explicitly stated in equation (4).

Based on the joint PDF $\hat{p}_{cw}(c,w;\bar{S})$ of equation (4) and the *Bartlett et al.* [2016] spatial description of threshold-excess and prethreshold runoff at a point, we derive an event-based model representation that is general to the PDFs of rainfall, $p_R(R)$, and storage capacity, $p_w(w)$ (see Appendix A). This point runoff description of *Bartlett et al.* [2016] consists of both prethreshold and threshold-excess runoff over the fraction of watershed area β, while over the complementary area, $1-\beta$, the point response only consists of threshold-excess runoff. The fraction β may represent riparian and lower hillslope areas with a persistent hydrologic connection to the stream that facilitates a prethreshold runoff before rainfall infiltration exceeds the storage capacity threshold. The complementary fraction of area $1-\beta$ may represent upslope areas where prethreshold runoff is zero because the connection to the stream episodically occurs when infiltration fills and then spills over the storage capacity threshold [*Bartlett et al.*, 2016].

2.3. Rainfall and Storage Capacity PDF Assumptions

Each new event-based model assumes a specific form of the storage capacity PDF, $p_w(w)$ (see Table 2). Typically, VIC and PDM both assume a Pareto distribution for the PDF $p_w(w)$, and so we refer to the extended event-based versions of VIC and PDM collectively as VICx/PDMx [*Moore*, 2007; *Liang et al.*, 1994]. Differently, in the case of TOPMODEL, $p_w(w)$ has a physical basis in the slope and contributing area at a point that define the topographic index, κ (see Appendix B). Over a watershed, the spatial distribution of the topographic index may be represented by the PDF $p_\kappa(\kappa)$. Here we represent $p_\kappa(\kappa)$ with an exponential PDF, and this PDF typically provides a good fit to the empirical distribution of the topographic index, especially for larger values that are representative of lowland areas where the majority of runoff production occurs according to the TOPMODEL concept (Appendix B). Starting from this exponential PDF, we derive the mirrored exponential PDF (Table 1) that reasonably represents the distribution of TOPMODEL storage capacity (see Appendix B).

For each storm event, we assume the spatial distribution of rainfall follows an exponential PDF, i.e.,

$$p_R(R) = \frac{1}{\bar{R}} e^{-R/\bar{R}}. \tag{6}$$

This PDF has been used to represent the spatial distribution of rainfall in small watershed areas of about 40 km^2 [*Yu*, 1998; *Schaake et al.*, 1996], as well as in climate and large-scale hydrologic models [*Thomas and*

Henderson-Sellers, 1991; *Liang et al.*, 1996; *Tang et al.*, 2007; *Sivapalan et al.*, 1997; *Shuttleworth*, 1988; *Arnell*, 2014, p. 279]. In the next sections, we assume the exponential rainfall PDF of equation (6) and the storage capacity PDFs of Table 2 and present the analytical expressions of the extended models of VICx/PDMx and TOPMODELx.

2.4. Fraction of Area With Threshold-Excess Runoff

For each event-based model, the fraction of area F_t represents the greatest extent of threshold-excess runoff at the end of a storm event. It is a fundamental quantity that forms the basis of the subsequent event-based model expressions. Following equation (A4), for VICx/PDMx the fraction of area with threshold-excess runoff is

$$F_t(\bar{S},\bar{R})=F(\bar{S})+\exp\left(-\frac{w_{\max}(1-F(\bar{S}))^\xi}{\bar{R}(1-P_I)}\right)\frac{1}{\xi}\left(-\frac{w_{\max}}{\bar{R}(1-P_I)}\right)^{-\frac{1}{\xi}}\left(\Gamma\left(\frac{1}{\xi}\right)-\Gamma\left(\frac{1}{\xi},\frac{-w_{\max}(1-F(\bar{S}))^\xi}{\bar{R}(1-P_I)}\right)\right), \quad (7)$$

where $\Gamma(\cdot)$ and $\Gamma(\cdot,\cdot)$ are the gamma and lower incomplete gamma functions, respectively [*Olver et al.*, 2010] (see Appendix C). For TOPMODELx, the fraction of area with threshold-excess runoff is

$$F_t(\bar{S},\bar{R})=F(\bar{S})+\frac{C_1\bar{R}(1-P_I)\xi}{\bar{R}(1-P_I)\xi-w_{\max}}\left(\left(\frac{F(\bar{S})}{C_1}+e^{-\xi}\right)^{\frac{w_{\max}}{\bar{R}(1-P_I)\xi}}-\left(\frac{F(\bar{S})}{C_1}+e^{-\xi}\right)\right). \quad (8)$$

For the SCS-CNx method the fraction of area $F_t(\bar{S},\bar{R})$ is given by *Bartlett et al.* [2016, equation (24)], where $\bar{S}=\bar{c}\bar{w}$ because c and w are statistically independent.

For equations (7) and (8), the first term is the fraction of area with threshold saturation prior to the storm, and the second term is the fraction of area where threshold-excess runoff develops during the storm. Over the complementary fraction of area $(1-F_t(\bar{S},\bar{R}))$, prethreshold runoff occurs over $\beta(1-F_t(\bar{S},\bar{R}))$ but is zero over $(1-\beta)(1-F_t(\bar{S},\bar{R}))$. The fraction of $F_t(\bar{S},\bar{R})$ varies with $\bar{S}$ (Figures 1a and 1b). Note that an increase in the prethreshold runoff area (an increase in β) decreases $F_t(\bar{S},\bar{R})$ and thus the extent of threshold-excess runoff over the watershed. When $P_I=0$, equations (7) and (8) of VICx/PDMx and TOPMODELx describe the extent of threshold-excess runoff when the prethreshold runoff is zero.

2.5. Runoff PDF

For each storm event, the runoff PDF represents the spatial variability of runoff depths that are cumulative values for the storm duration. Following equation (A5), this PDF is the weighted sum of the prethreshold and threshold-excess runoff PDFs of equations (C1–C4). For the exponential rainfall PDF and no prethreshold runoff ($\beta=0$ and $P_I=0$), the runoff PDF has a remarkably simple form for all models, i.e.,

$$p_Q(Q)=(1-F_t(\bar{S},\bar{R}))\delta(Q)+\frac{F_t(\bar{S},\bar{R})}{\bar{R}}e^{\frac{-Q}{\bar{R}}}, \quad (9)$$

where $F_t(\bar{S},\bar{R})$ is that of either equations (7) and (8) or *Bartlett et al.* [2016, equation (24)] for the SCS-CNx method. In equation (9), runoff is zero over the fraction of area $1-F_t(\bar{S},\bar{R})$ as represented by the point mass of probability $(1-F_t(\bar{S},\bar{R}))\delta(Q)$, while the runoff depths are exponentially distributed over the fraction of area $F_t(\bar{S},\bar{R})$ as represented by PDF of the second term.

For the general case of $\beta\neq0$, the prethreshold runoff contributes to the probability density for smaller runoff values (Figure 2, dashed line and bar), while the threshold-excess runoff contributes more to the probability density for larger runoff values (Figure 2, gray line). As a result, the expressions are not as simple as equation (9), but are still exact expressions as shown in Appendix C. Note the black bars of Figure 2 represent the fraction of area that produces zero runoff as indicated by the atom of probability $(1-F_t(\bar{S},\bar{R}))(1-\beta)\delta(Q)$, which is the first term of prethreshold runoff PDFs weighted by $1-F_t(\bar{S},\bar{R})$ (see equations (C1) and (C2)).

2.6. Average Runoff (the Runoff Curve)

The key result is an expression of the average runoff $\bar{Q}$ as a function of average rainfall, $\bar{R}$, and the average antecedent potential retention, $\bar{S}$, the so-called "runoff-curve." While the extended SCS-CNx method, VICx/PDMx, and TOPMODELx are based on different assumptions, each model has the same basic runoff curve expression, i.e.,
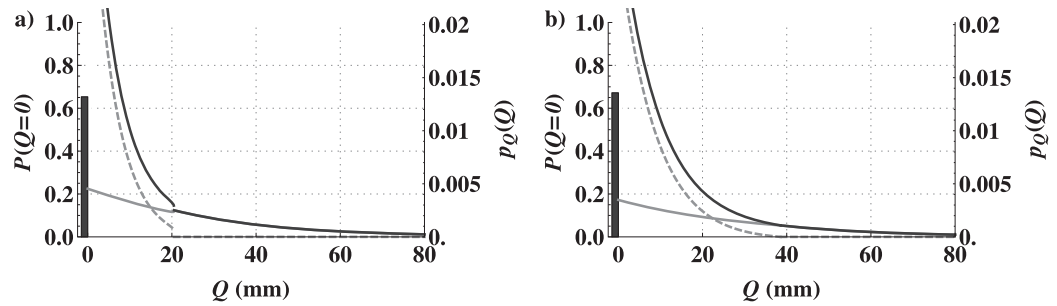
Figure 2. The runoff PDFs for (a) VICx/PDMx and (b) TOPMODELx, respectively, when $\bar{S}=70$ and $\bar{R}=25$ mm, which consists of a continuous probability density (right axis, solid line) and an atom of probability for $Q=0$ (left axis, black bar). In both cases the PDF is the total of the weighted prethreshold runoff PDF (dashed line and black bar), i.e., $(1-F_t(\bar{S},\bar{R}))p_{Q_p}(Q)$, plus the weighted threshold-excess runoff PDF (gray line), i.e., $F_t(\bar{S},\bar{R})p_{Q_t}(Q)$ (Appendix C). See Table 3 for parameters values, and here we assume $\beta=0.25$.

$$\bar{Q}=\bar{R}F_t(\bar{S},\bar{R})+\bar{R}(1-F_t(\bar{S},\bar{R}))P_I. \tag{10}$$

The exact forms of each runoff curve differ based on the function $F_t(\bar{S},\bar{R})$. The runoff curve of equation (10) is the first of its kind for describing an event-based semidistributed runoff response consisting of both threshold-excess runoff generated on the fraction of area $F_t(\bar{S},\bar{R})$ and the prethreshold runoff originating from the complementary fraction of area $1-F_t(\bar{S},\bar{R})$. When $P_I=0$, the runoff curve defaults to $\bar{R}F_t(\bar{S},\bar{R})$, which describes the runoff response of the original models, but in an event-based format. Note that for $P_I = \beta(1-\bar{c})$, $\bar{c}$ may be given in terms of $\bar{S}$ (see Table 2).

Following equation (A8), the average runoff of equation (10) is the weighted sum of the average prethreshold and threshold-excess runoff components given by equations (C5–C8). As the average rainfall increases, the average runoff also increases (Figure 3), with higher amounts of runoff being produced as the watershed nears saturation, i.e., $\bar{S}$ approaches 0 (Figure 3). The behavior of the prethreshold runoff augments threshold-excess runoff and increases the total average runoff, especially for smaller values of average rainfall (Figure 3). Although the majority of the runoff is threshold-excess runoff (Figure 3), the area of threshold-excess runoff typically comprises a small area of the watershed (e.g., less than 50%). This is especially true as the amount of prethreshold runoff increases (i.e., as β approaches 1) because the prethreshold runoff acts as a drainage mechanism for the watershed that decreases the soil water content and thus the occurrence of threshold-excess runoff.

3. Analysis of the Event-Based Models

3.1. Case Study Area and Data
To analyze the model behavior, we use data from the Davidson river watershed, which consists of approximately 104 km² near Brevard, North Carolina, USA. At the watershed outlet, streamflow is recorded by the
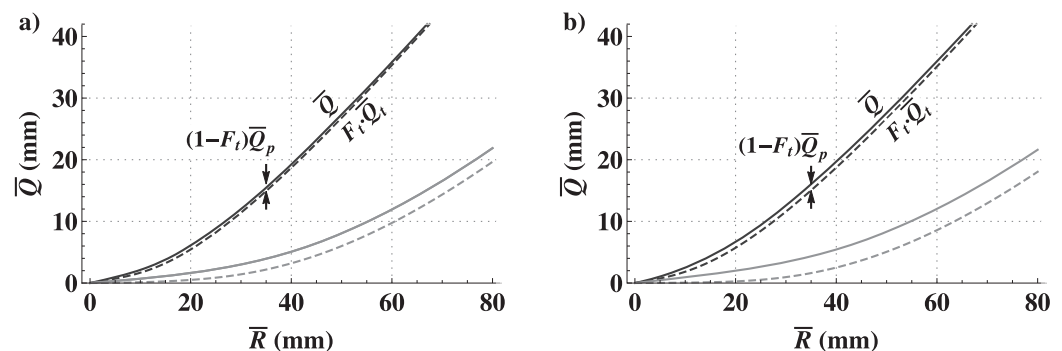

Figure 3. The average runoff, $\bar{Q}$ (solid lines) versus the average rainfall, $\bar{R}$ for (a) VICx/PDMx and (b) TOPMODELx. The average runoff is the weighted sum of the average threshold-excess runoff, $F_t(\bar{S},\bar{R})\bar{Q}_t$ (dashed lines), and the average prethreshold runoff $(1-F_t(\bar{S},\bar{R}))\bar{Q}_p$; see Appendix C. Cases are shown for $\bar{S}=35$ (black lines), and $\bar{S}=123$ (gray lines). See Table 3 for parameter values.
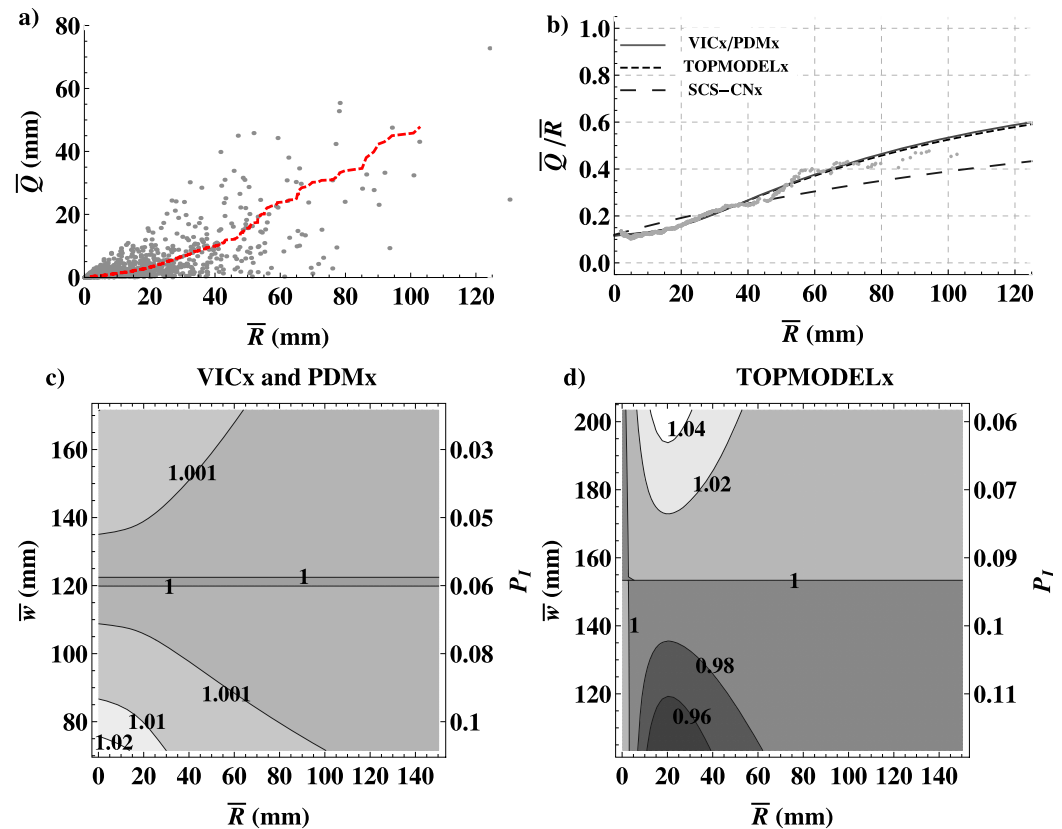
Figure 4. For the Davidson River, (a) the rainfall-runoff data (gray dots) and rank-order data runoff curve (red dashed line) and (b) a comparison the rank-order data runoff coefficients (gray dots) to the models (lines) for the $\bar{S}$ and P_I of Table 3. For the parameters of Table 3 contours indicate the ratio of $\bar{Q}$ for different $\bar{w}$ (and P_I) to $\bar{Q}$ for constant values of (c) $\bar{w} = 122$ mm (and $P_I = 0.061$) for VICx and PDMx and (d) $\bar{w} = 153$ mm (and $P_I = 0.088$) for TOPMODELx. Note that $\bar{w}$ and P_I satisfy $0.12 = F(\bar{S}) + P_I$ where 0.12 is the initial runoff coefficient of the data and $F(\bar{S})$ is dependent on $\bar{w}$ (Table 2).

United States Geological Survey (USGS) gauge 03441000. Daily rainfall values are measured by the nearest USGS rain gauge (03455773) that is located 19 km away at Lake Logan. A 3 m resolution digital elevation model (DEM) downloaded from the National Elevation Dataset (ned.usgs.gov) describes the topography of the watershed. From this DEM, we computed the topographic index with the TauDEM D-Infinity tools [*Tarboton and Mohammed*, 2013], and clipped the resulting values to the Davidson River area using the Watershed Boundary Dataset (nhd.usgs.gov, HUC12, 060101050202).

We examined Davidson river streamflow and rainfall data between 1 December 1998 and 11 November 2015, and only considered storm events where rainfall exceeded 2 mm. Rainfall values are cumulative totals for each storm event, and we assume each storm may consist of up to three consecutive daily values. For each storm, we separated stormflow values from the USGS measured streamflow using the hydrograph separation program (HYSEP) [*Sloto and Crouse*, 1996; *Eckhardt*, 2008]. Runoff values also are cumulative totals that are found by integrating the stormflow over the duration of each storm event. The period of record (6196 days) contained 1212 rainfall-runoff events with an average rainfall of $\langle \bar{R} \rangle = 15.5$ mm and average runoff of $\langle \bar{Q} \rangle = 4.1$ mm (Figure 4a).

In addition, we rank-ordered the rainfall-runoff data by pairing respective lists of the rainfall and runoff values that have been sorted in descending order. In this way, the rainfall-runoff data are matched by frequency, and consequently runoff typically is no longer matched with the causative rainfall event. However, for the period of record, this rank-order data approximately represents the rainfall-runoff response (i.e., the runoff curve) for average watershed conditions, i.e., $\bar{S} \approx \langle \bar{S} \rangle$ (Figure 4a, dashed red line) [see *Bartlett et al.*, 2016, Appendix D]. We reduce the number of parameters by substituting $P_I = 0.12 - F(\bar{S})$ where 0.12 is the initial runoff coefficient for small rainfall events between 2 and 5 mm (Table 3). The remaining parameters (i.e.,

Table 3. Model Parameters and RMSE Comparison for the Davidson River Rank-Order Data

	VICx/PDMx	TOPMODELx	SCS-CNx	Unit	Description
$\bar{S}$	68[a]	71[a]	198[a]	mm	Average antecedent potential retention
P_I	0.06[a]	0.088[a]	0.12[a]		Prethreshold runoff index
w_{max}	137[a]	182[a]	∞	mm	Maximum point storage capacity and PDF scale parameter (Table 2)
ξ	8.42[a]	6.3[b]			Shape parameter of storage capacity PDF (Table 2)
κ_{max}		12.5[c]			Max. topographic index
κ_{min}		3.2[d]			Min. topographic index
κ_s		1.48[d]			Parameter of topographic index PDF (see equation (B4))
RMSE	0.012	0.011	0.033		Root mean square error between data and model runoff coefficients

[a]Nonlinear least squares fit of equation (10) to rainfall-runoff data after substituting $P_I = 0.12 - F(\bar{S})$ where 0.12 is the initial runoff coefficient for rainfall between 2 and 5 mm.
[b]Parameter is equal to $\xi = \frac{\kappa_{max} - \kappa_{min}}{\kappa_s}$ (see Appendix B).
[c]Value for which 95.5% topographic index values, κ, are between $0 < \kappa < \kappa_{max}$. Values between $\kappa_{max} < \kappa < \infty$ represent stream channel areas that occupy 0.5% of the watershed based on a drainage density of $D = 6.26 \text{ mi}^{-1}$ [*Carlston*, 1963] and an average stream channel width of $C_w = 4.5$ ft [*Chapman*, 1996, p. 248], i.e., $0.005 = DC_w$.
[d]Nonlinear least squares fit of the cumulative distribution function (CDF) $C_1 - C_1 \exp\left(\frac{-\kappa + \kappa_{min}}{\kappa_s}\right)$ to the empirical cumulative distribution of the topographic index. The CDF corresponds to the PDF of equation (B4).

w_{max}, ξ, and $\bar{S}$) are based on a nonlinear least squares fit of each model runoff curve to the rank-order (Table 3). In the case of TOPMODEL, the PDF shape parameter ξ is derived from topographic index parameters that are found from a nonlinear least squares fit of an exponential cumulative distribution function (CDF) to the empirical distribution of the topographic index (Appendix B and Table 3).

3.2. Data and Model Behavior Comparison

We initially compare each model runoff curve to the rank-ordered data and discuss how the runoff curve may relate to different basin attributes. Second, we compare the model runoff curves under different rainfall and antecedent wetness scenarios, and we relate the model differences to the spatial variability of the runoff response. The model runoff curves (equation (10)) and rank-ordered data are compared in terms of runoff coefficients, $\bar{Q}/\bar{R}$ (Figure 4b). Each of the fitted models reproduces the rainfall-runoff event behavior with a small root mean squared error (RMSE) (Figure 4 and Table 3). Both VICx/PDMx and TOPMODELx provide a better fit to the data than the SCS-CNx method. In comparison to VICx/PDMx and TOPMODELx, the SCS-CNx method predicts a larger runoff coefficient for smaller rainfall events, while predicting a smaller runoff coefficient for larger rainfall events. This difference results from different PDFs $\hat{p}_{cw}(c, w; \bar{S})$ assumed for watershed variability.

Each model (Figure 4b) represents the rainfall-runoff response curve for a storm event defined by the Table 3 values of ξ, w_{max}, $\bar{S}$, and P_I. In each model, the initial runoff coefficient of the data (i.e., 0.12) is equal to $F(\bar{S}) + P_I$. Since $F(\bar{S})$ is dependent on $\bar{w}$ (see Table 2), many combinations of $\bar{w}$ and P_I result in approximately similar average runoff values (Figures 4c and 4d), which is the so-called problem of "equifinality" [*Beven*, 2006]. Consequently, the same storm event runoff $\bar{Q}$ could result from a shallower basin (smaller $\bar{w}$) that produces more threshold-excess runoff but less prethreshold runoff, or it could result from a deeper basin (larger $\bar{w}$) that produces less threshold-excess runoff but more prethreshold runoff. While $\bar{Q}$ would be similar, the spatial description of runoff would be different. Thus fitting each model to a single storm event requires both rainfall-runoff data and other process information such as the mapped near stream saturated area.

For small rainfall events over the Davidson river basin, the SCS-CNx method produces more runoff than either VICx/PDMx (Figure 5a) or TOPMODEL (Figure 5b). The greatest differences between the SCS-CNx method and either VICx/PDMx or TOPMODELx occurs for rainfall between $0 < \bar{R} < 50$ mm, and the magnitude of the differences decreases with $\bar{S}$ (Figure 5). In wetter conditions (e.g., $\bar{S} < 50$), the runoff predictions of the SCS-CNx method, VICx/PDMx, and TOPMODELx become more similar, but under drier conditions (e.g., $\bar{S} > 50$), the SCS-CNx method may predict 4 times more runoff than TOPMODELx and nearly 5 times more runoff than VICx/PDMx (Figures 5a and 5b).

Differences in the average runoff response (Figures 5a and 5b) are mainly attributed to differences in the fraction of area with threshold-excess runoff, $F_t(\bar{S}, \bar{R})$. The behavior of $F_t(\bar{S}, \bar{R})$ with rainfall is different for each model because of difference in the joint PDF $\hat{p}_{cw}(c, w; \bar{S})$. Specifically, within this joint PDF, the
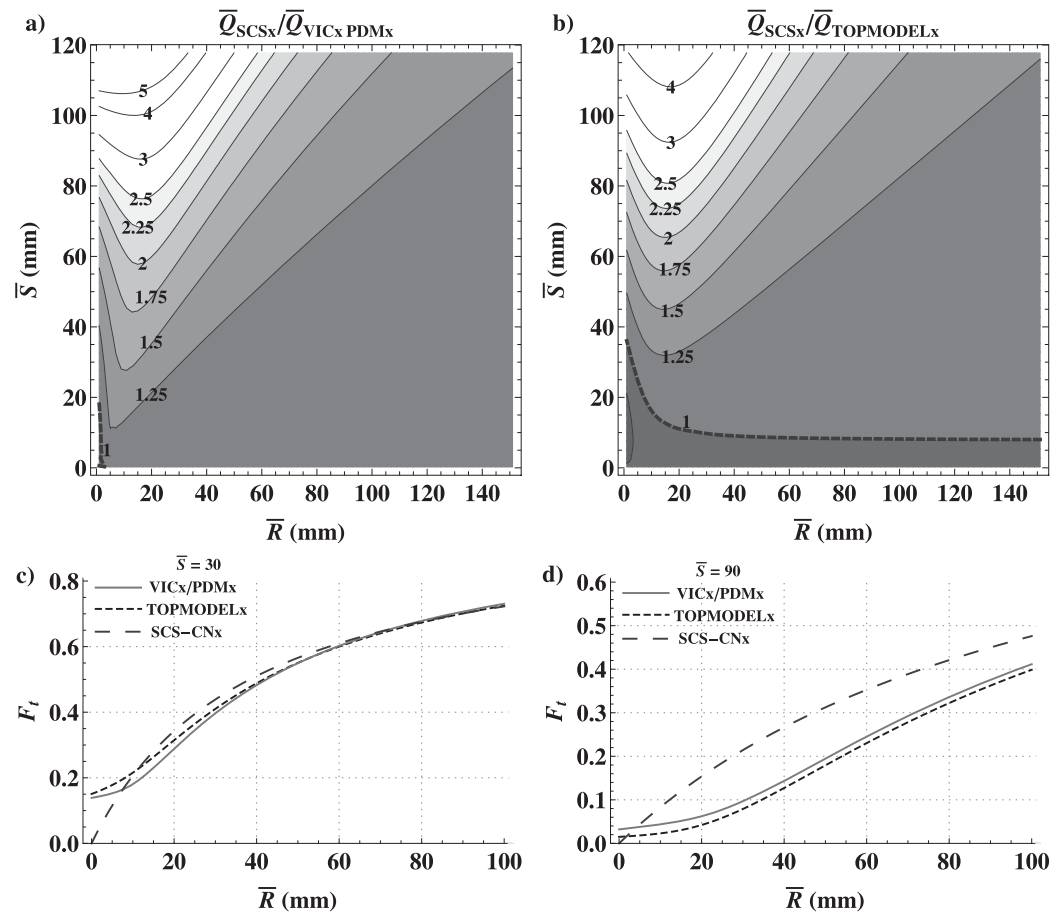
Figure 5. Contours indicate the ratio of SCS-CNx method runoff, $\bar{Q}_{SCSx}$, to (a) VICx/PDMx runoff, $\bar{Q}_{VICxPDMx}$, and (b) TOPMODELx runoff, $\bar{Q}_{TOPMODELx}$. The fraction of area with threshold-excess runoff for (c) $\bar{S}=30$ and (d) $\bar{S}=90$. See Table 3 for parameter values for which the fraction β is equal to 0.085 and 0.16 for VICx/PDMx and TOPMODELx, respectively, and 0.24 for the SCS-CNx method assuming $\bar{w}=400$ mm.

marginal storage capacity PDF, $p_w(w)$ is skewed toward smaller storage capacity values for the SCS-CNx method, but for the Davidson river case study area, the distribution is skewed toward larger values for VICx/PDMx and TOPMODELx (Figures 5c and 5d). Under wetter conditions (e.g., $\bar{S}=30$), the models tend to have similar values of $F_t(\bar{S},\bar{R})$, while under drier conditions (e.g., $\bar{S}=90$), the differences in $F_t(\bar{S},\bar{R})$ tend to be greater (Figures 5c and 5d).

4. Discussion

4.1. Unified and Extended Semidistributed Models
The main contribution of this work is the development of a general expression for the average runoff (i.e., the rainfall-runoff curve) that unifies the different modeling approaches of the SCS-CN method, VIC, PDM, and TOPMODEL. These general expressions includes both prethreshold and threshold-excess runoff components over the respective fractions of area $(1-F_t(\bar{S},\bar{R}))\beta$ and $F_t(\bar{S},\bar{R})$. Each runoff area is modeled with a distribution of storage capacity thresholds where each local threshold may act as a proxy for many different rainfall-runoff mechanisms, e.g., subsurface flow and overland flow by saturation of infiltration excess [*Bartlett et al.*, 2016; *McDonnell*, 2013]. Aside from the expression for $F_t(\bar{S},\bar{R})$, the spatial variability of prethreshold and threshold-excess runoff is also represented by the runoff PDF $p_Q(Q)$. This spatial characterization of runoff is further enhanced by the fact that each model accounts for the spatial distribution of rainfall with the exponential PDF of equation (6). For all models, the fraction of area β and the average antecedent potential retention, $\bar{S}$, govern the magnitude and spatial extent of the runoff response.

According to the original semidistributed runoff concept [*Beven and Kirkby*, 1979, equation (9); *Moore*, 1985, equation (3); *Wood et al.*, 1992, equations (3a) and (3b); *Kavetski et al.*, 2003, equation (2)], the runoff rate at time t is given by $\bar{Q}(t) = \bar{R}(t)F(\bar{S}(t))$, where $\bar{R}(t)$ is the rainfall rate and the saturated area $F(\cdot)$ of Table 2 is a function of the average potential retention at time t. The equivalent event-based form, $\bar{Q} = \bar{R}F_t(\bar{S}, \bar{R})$, is given by the general runoff curve of equation (10) when $\beta = 0$. It is important to note that this form is similar to the original concept of runoff production over a saturated area, but now $\bar{R}$ and $\bar{Q}$ represent cumulative totals for the storm event, $\bar{S}$ is an antecedent value immediately prior to the storm, and $F_t(\cdot, \cdot)$ is the threshold-saturated area immediately after the storm, which depends on both $\bar{R}$ and $\bar{S}$. The new general rainfall-runoff curve of equation (10) also is extended with prethreshold runoff that occurs over the fraction of the watershed β. By accounting for this prethreshold runoff, each model now may capture runoff from smaller rainfall events that do not activate large areas of threshold-excess runoff. Thus, by calibrating the prethreshold runoff index, P_I, each model may represent watersheds with more storage, i.e., a large $\bar{w}$, where small rainfall events produce less threshold-excess runoff. The models extended with the prethreshold runoff flux may better represent the runoff response over a variable source area (VSA) that consists of a lateral flux of water (via macropores and other organized flow pathways) to a saturated area [e.g., *Hewlett and Hibbert*, 1967].

4.2. Ungauged Basin Predictions

The traditional SCS-CN method is an event-based model that is widely used for ungauged basin predictions because the single parameter $\bar{S}$ is defined by a dimensionless curve number (CN) listed in tables according to the watershed soil type, hydrologic condition, and land use type [*Bartlett et al.*, 2016; *USDA National Resources Conservation Service*, 2004]. However, SCS-CN method predictions are only appropriate for ungauged watersheds that match its general assumptions, i.e., zero prethreshold runoff, $P_I = 0$, and the specific form of its PDF $\hat{p}_{cw}(c, w; \bar{S})$ [see *Bartlett et al.*, 2016, equation (23)]. These assumptions are limited largely to the agricultural watersheds that informed the empirical development of the SCS-CN method. The assumptions for $P_I = 0$ and the PDF $\hat{p}_{cw}(c, w; \bar{S})$ may be different for nonagricultural watersheds, which may be represented by the PDFs of $\hat{p}_{cw}(c, w; \bar{S})$ that are specific to semidistributed models. Furthermore, any number of different PDFs may be assumed, and for each new PDF $\hat{p}_{cw}(c, w; \bar{S})$, a new event-based model may be created by following the ProStor framework.

4.3. Watershed Heterogeneities

For each model, the PDF $\hat{p}_{cw}(c, w; \bar{S})$ represents the distribution of thresholds described by the soil moisture deficit, c, and the storage capacity, w, where points in the fraction of area β also have a prethreshold runoff. In turn, the PDF $\hat{p}_{cw}(c, w; \bar{S})$ and the fraction β govern the rainfall-runoff response of each model. However, in an actual watershed, the rainfall-runoff is governed by physical heterogeneities such as (1) soil macropore networks, soil layering, and other organized flow behavior; (2) plant root distributions and the corresponding soil water uptake; (3) bedrock topography and bedrock composition; and the (4) spatial patterns of soil moisture [*McDonnell et al.*, 2007]. Many of these heterogeneities are not easily observed; thus, it is difficult to explicitly characterize a watershed from available data. However, such heterogeneities are primarily responsible for the phenomenological emergence of watershed storage thresholds [*McDonnell*, 2013; *Tromp-van Meerveld and McDonnell*, 2006a,b]. Thus, aside from the storage capacity and antecedent soil moisture deficit, the PDF $\hat{p}_{cw}(c, w; \bar{S})$ may implicitly represent many different types of watershed heterogeneities. In addition, at larger scales, different watershed heterogeneities may define the extent of the fraction of the watershed β that produces prethreshold runoff. Consequently, both $\hat{p}_{cw}(c, w; \bar{S})$ and β may provide a way to characterize the heterogeneous structure of a watershed. In the future, the ProStor framework and resulting event-based models could be practically applied for understanding the link between joint distributions of watershed heterogeneities and regional and ecological factors (e.g., climate and land use). Such links could be revealed through an extensive analysis of different watersheds that compares factors (regional and ecological) with the distributions that provide the optimal runoff curve for capturing historic rainfall-runoff data.

5. Concluding Remarks

We have distilled the semidistributed modeling approaches of VIC, PDM, and TOPMODEL into event-based models consisting of a basic set of ready-to-use analytical expressions that describe the rainfall-runoff

response. These expressions are for the runoff PDF that describes the spatial variability of runoff, the fractions of watershed that are the source of runoff by a specific mechanism, and the average (unit area) runoff (i.e., the runoff curve). These expressions represent the first event-based description of each modeling approach. We have also shown that the event-based semidistributed models and the SCS-CN method are united by the same general expression for the runoff curve. This general expression for the resulting models of VICx, PDMx, TOPMODELx, and SCS-CNx is extended with a new runoff concept based on thresholds that now accounts for prethreshold runoff that varies with the parameter called the prethreshold runoff index. By calibrating this parameter, the event-based models may capture runoff from storms that do not activate large areas of threshold-excess runoff [e.g., *Bartlett et al.*, 2015, 2016].

Comparisons of these different models previously required more time-consuming numerical simulations. However, with the new analytical expressions, the runoff behavior of each model now may be compared on an event-basis. These analytical expressions can be used in existing models to simplify storm rainfall with an event-based representation that also provides an implicit characterization of the spatial variability of runoff. This spatial characterization may improve predictions of runoff-mediated processes such as erosion or pollutant transport. Furthermore, the model expressions may be easily interchanged in calculations and models that operate according to an event-based runoff curve. For example in the soil and water assessment tool (SWAT) model [*Saleh et al.*, 2000], the new expressions for VICx/PDMx, TOPMODELx, or SCS-CNx easily could be substituted for the runoff curve of the traditional SCS-CN method, which may be beneficial since different runoff models may provide better performance for certain watershed types [e.g., *Clark et al.*, 2008]. In addition, the analytical expressions incorporate assumptions for the rainfall-runoff response at a point and the distribution of storage capacity and soil moisture. Thus, these expressions may facilitate comparisons between model assumptions and regional and ecohydrological factors such as land use, site type, and climate conditions.

Appendix A: General Event-Based Rainfall-Runoff Model

Following the ProStor framework, we now assume a point rainfall-runoff response for equation (2) and derive an event-based model that is specific to the VIC/PDM and TOPMODEL assumption for the joint PDF $\hat{p}_{cw}(c, w; \bar{S})$ of equation (4). The resulting model is general to the PDFs of storage capacity, $p_w(w)$, and rainfall, $p_R(R)$.

A1. Rainfall-Runoff Response at a Point

For the rainfall-runoff response at a point, *Bartlett et al.* [2016] considered two different threshold descriptions. Over a fraction of watershed area β, runoff occurs both before and after infiltration exceeds the storage capacity threshold, w, i.e., [see *Bartlett et al.*, 2016, Figure 1]

$$Q_1(R, c, w) = \begin{cases} R\bar{x} & \text{for} \quad 0 \leq R < \dfrac{cw}{1-\beta\bar{x}} \\[3mm] R - cw\dfrac{1-\bar{x}}{1-\beta\bar{x}} & \dfrac{cw}{1-\beta\bar{x}} \leq R < \infty \end{cases}. \tag{A1}$$

The "prethreshold" runoff $R\bar{x}$ is controlled by the watershed wetness, i.e., the average antecedent soil moisture $\bar{x} = 1 - \bar{c}$.

Over the complementary fraction of watershed area, $1-\beta$, runoff only occurs when infiltration exceeds the storage capacity threshold, i.e.,

$$Q_2(R, c, w) = \begin{cases} 0 & \text{for} \quad 0 \leq R < \dfrac{cw}{1-\beta\bar{x}} \\[3mm] R - \dfrac{cw}{1-\beta\bar{x}} & \dfrac{cw}{1-\beta\bar{x}} \leq R < \infty \end{cases}. \tag{A2}$$

When $\beta = 0$ this fraction of area describes the original point runoff concept of the SCS-CN method, VIC, PDM, and TOPMODEL. For both equations (A1) and (A2), infiltration at a point is $R - \beta R\bar{x}$, i.e., rainfall minus the spatial average of prethreshold runoff over the watershed. This infiltration, $R - \beta R\bar{x}$, equals the

antecedent potential retention, cw, when $R=\frac{cw}{1-\beta\bar{x}}$. This formulation for infiltration accounts for the intra-storm lateral moisture redistribution from the fraction of area $1-\beta$ to the fraction of area β. Consequently, for points on the boundary between β and $1-\beta$, the soil moisture deficit is the same.

A2. Spatially Lumped Response

The rainfall-runoff responses of equations (A1) and (A2) are substituted into equation (3) to find respective joint PDFs $p_{Q_1 Rcw}(Q,R,c,w)$ and $p_{Q_2 Rcw}(Q,R,c,w)$. The PDF $p_{QRcw}(Q,R,c,w)$ for the entire area is the weighted sum $\beta p_{Q_1 Rcw}(Q,R,c,w)+(1-\beta)p_{Q_2 Rcw}(Q,R,c,w)$, where for VIC/PDM and TOPMODEL $\hat{p}_{cw}(c,w;\bar{S})$ is given by equation (4), i.e.,

$$
p_{QRcw}(Q,R,c,w)=
\begin{cases}
(\beta\delta(R\bar{x}-Q)+(1-\beta)\delta(Q)) & \text{for} \quad 0\leq R<\dfrac{cw}{1-\beta\bar{x}} \\[2ex]
\delta\left(cw-w+P_w^{-1}[F(\bar{S})]\right)p_w(w)p_R(R) & P_w^{-1}[F(\bar{S})]\leq w<w_{\max} \\[4ex]
\left(\beta\delta\left(R-\dfrac{cw(1-\bar{x})}{1-\beta\bar{x}}-Q\right)\right. & \dfrac{cw}{1-\beta\bar{x}}\leq R<\infty \\[2ex]
\left.+(1-\beta)\delta\left(R-\dfrac{cw}{1-\beta\bar{x}}-Q\right)\right)\delta(c)p_w(w)p_R(R) & 0\leq w<P_w^{-1}[F(\bar{S})] \\[4ex]
\left(\beta\delta\left(R-\dfrac{cw(1-\bar{x})}{1-\beta\bar{x}}-Q\right)\right. & \dfrac{cw}{1-\beta\bar{x}}\leq R<\infty \\[2ex]
\left.+(1-\beta)\delta\left(R-\dfrac{cw}{1-\beta\bar{x}}-Q\right)\right) & P_w^{-1}[F(\bar{S})]\leq w<w_{\max} \\[2ex]
\delta\left(cw-w+P_w^{-1}[F(\bar{S})]\right)p_w(w)p_R(R), &
\end{cases}
\tag{A3}
$$

where the first term represents the variability of prethreshold runoff, the second term represents the variability of runoff from the fraction of watershed area with threshold saturation prior to the storm, $F(\bar{S})$, and the third term represents the variability of threshold-excess runoff that develops during the storm. For equation (A3), integration over the Dirac delta functions, $\delta(\cdot)$, is performed using the property discussed in *Au and Tam* [1999] and *Bartlett et al.* [2016, Appendix E].

The source area of threshold-excess runoff is equal to the integral of $p_R(R)p_{cw}(c,w)$ over the range $\frac{cw}{1-\beta\bar{x}}\leq R<\infty$ where threshold-excess runoff occurs. In this case, it is equal to the sum of two terms: (1) the fraction of watershed area with threshold saturation prior to the storm, $F(\bar{S})$, for the range $0<w<P_w^{-1}[F(\bar{S})]$ and (2) the fraction of watershed area that develops threshold saturation during the storm for the range $P_w^{-1}[F(\bar{S})]\leq w\leq w_{\max}$, i.e.,

$$
F_t(\bar{S},\bar{R})=F(\bar{S})+\int_{P_w^{-1}[F(\bar{S})]}^{w_{\max}}\int_{\frac{w-P_w^{-1}[F(\bar{S})]}{1-\beta\bar{x}}}^{\infty}p_R(R)p_w(w)dRdw.
\tag{A4}
$$

Note that equation (A4) may also be stated as

$$
F_t(\bar{S},\bar{R})=1.-\int_0^{\frac{w_{\max}-P_w^{-1}[F(\bar{S})]}{1-\beta\bar{x}}}\int_{R(1+\beta\bar{x})+P_w^{-1}[F(\bar{S})]}^{w_{\max}}p_R(R)p_w(w)dwdR.
$$

When $\beta=0$, runoff is not produced over $1-F_t(\bar{S},\bar{R})$ since the only runoff mechanism is threshold-excess; however, when $\beta\neq0$, runoff is produced over $1-F_t(\bar{S},\bar{R})$ by the prethreshold runoff mechanism.

The PDF of runoff, $p_Q(Q)$, may be written as a combination of the PDFs for the prethreshold runoff, $p_{Q_p}(Q)$, runoff and the threshold-excess runoff, $p_{Q_t}(Q)$, i.e.,

$$p_Q(Q) = (1 - F_t(\bar{S}, \bar{R}))p_{Q_p}(Q) + F_t(\bar{S}, \bar{R})p_{Q_t}(Q). \tag{A5}$$

The fraction of prethreshold area is the normalization constant for the prethreshold runoff PDF, i.e.,

$$p_{Q_p}(Q) = (1 - \beta)\delta(Q) + \frac{1}{1 - F_t(\bar{S}, \bar{R})}\left(\frac{\beta}{\bar{x}}p_R\left(\frac{Q}{\bar{x}}\right)\int_{P_w^{-1}[F(\bar{S})]+\frac{Q(1-\beta x)}{\bar{x}}}^{w_{max}} p_w(w)dw\right), \tag{A6}$$

where the first term represents the discrete probability of zero runoff and the second term represents a continuous range of runoff values between $0 < Q < L(\bar{S})$. In equation (A6), the delta function in the first term represents an atom of probability for zero prethreshold runoff over the fraction of area, $1 - \beta$, while the continuous PDF of the second term represents the variability of prethreshold runoff over the fraction of area, β.

The fraction of area $F_t(\bar{S}, \bar{R})$ is the normalization constant for the threshold-excess runoff PDF, i.e.,

$$p_{Q_t}(Q) = \frac{1}{F_t(\bar{S}, \bar{R})}\left(F(\bar{S})p_R(Q) + (1 - \beta\bar{x})(1 - \beta)\int_Q^{Q+\frac{L(\bar{S})\beta}{P_l}} p_R(R)p_w\left((R-Q)(1-\beta\bar{x}) + P_w^{-1}[F(\bar{S})]\right)dR\right.$$

$$+ C_2\beta\int_Q^{Q+\frac{L(\bar{S})(1-P_l)\beta}{C_2P_l}} p_R(R)p_w\left((R-Q)C_2 + P_w^{-1}[F(\bar{S})]\right)dR \tag{A7}$$

$$\left.- C_2\beta\int_{\frac{Q}{\bar{x}}}^{Q+\frac{L(\bar{S})(1-P_l)\beta}{C_2P_l}} p_R(R)p_w\left((R-Q)C_2 + P_w^{-1}[F(\bar{S})]\right)dR\right),$$

where the first term represents threshold-excess runoff between $0 \leq Q < \infty$ over the antecedent fraction of watershed with threshold saturation, $F(\bar{S})$, and the second, third, and fourth terms collectively represent threshold-excess runoff over areas that develop threshold saturation during the storm. Note that the second and third terms represent runoff between $0 < Q < \infty$, while the fourth term is for runoff between $0 < Q < L(\bar{S})$ and subtracts the probability density over the integration region for prethreshold runoff (see Figure 6). Equation (A7) may be integrated by using a change of variables, i.e., $R^* = R(1 - P_l)$ and $Q^* = Q(1 - P_l)$ or $R^* = RC_2$ and $Q^* = QC_2$ (see Table 4).

The average (unit area) runoff is the sum of the average prethreshold runoff weighted by $1 - F_t(\bar{S}, \bar{R})$ plus the average threshold-excess runoff weighted by $F_t(\bar{S}, \bar{R})$, i.e.,

$$\bar{Q} = (1 - F_t(\bar{S}, \bar{R}))\int_0^{L(\bar{S})} Qp_{Q_p}(Q)dQ + F_t(\bar{S}, \bar{R})\int_0^\infty Qp_{Q_t}(Q)dQ, \tag{A8}$$

where for $\beta = 0$, the first term of equation (A8) is zero because $p_{Q_p}(Q) = \delta(Q)$.
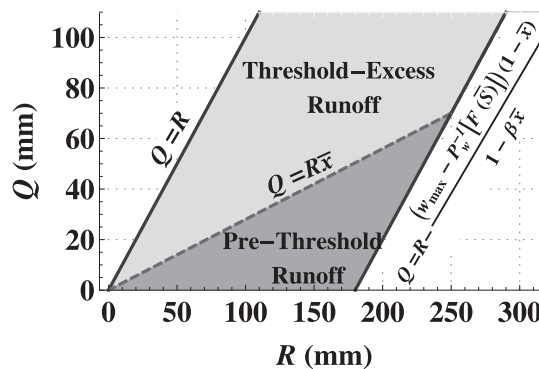

Figure 6. For the third and fourth terms of equation (A7), the threshold-excess runoff region of integration (light gray) and the pre-threshold runoff region of integration (dark gray) for $\beta = 0.35$, $\bar{x} = 0.8$, and $w = 200$ mm. The boundary between the two regions (dashed line) is given by the general threshold description of equation (A1) when $R = (cw)/(1 - \beta\bar{x})$.

Appendix B: TOPMODEL Storage Capacity Distribution

For TOPMODEL, each point storage capacity, w, is based on a topographic index value given by

$$\kappa = \ln\left(\frac{a}{\tan(S_l)}\right), \tag{B1}$$

where a is the upslope contributing area per unit contour length, and S_l is the topographic slope. The topographic index is often referred to as a similarity index because points with the same topographic index are assumed to have a similar hydrologic response [*Beven and Kirkby*, 1979]. TOPMODEL uses the topographic index distribution to calculate the catchment hydrologic response without considering every point individually.

Table 4. Functions and Constants

Symbol	Expression[a,b]
$L(\bar{S})=$	$\frac{P_l(w_{max}-P_w^{-1}[F(\bar{S})])}{(1-P_l)\beta}$
$M(\bar{S})=$	$(1-F(\bar{S}))^{\xi}$
$N(\bar{S})=$	$\frac{F(\bar{S})}{C_1}+e^{-\xi}$
$C_1=$	$\frac{1}{1-e^{-\xi}}$
$C_2=$	$\frac{(1-P_l)\beta}{\beta-P_l}$

[a]The prethreshold loss index is $P_l=\beta(1-\bar{c})$. See Tables 2 and 3 for other parameter definitions.
[b]For TOPMODEL, $\xi=\frac{\kappa_{max}-\kappa_{min}}{\kappa_s}$ (see Table 2).

The topographic index, κ, and the storage capacity, w, are related by the expression

$$w=w_{max}\frac{\kappa_{max}-\kappa}{\kappa_{max}-\kappa_{min}}, \qquad (B2)$$

where $0\le w\le w_{max}$ and watershed area has values $\kappa_{min}<\kappa<\kappa_{max}$ [*Sivapalan et al.*, 1997]. The minimum topographic index value k_{min} corresponds to a maximum reservoir depth of w_{max}, while the maximum topographic index value, k_{max} corresponds to a minimum reservoir depth, which for simplicity, we consider to be zero [*Sivapalan et al.*, 1997].

The TOPMODEL storage capacity distribution is represented by the mirrored exponential PDF (Table 2). This PDF is the marginal of the joint PDF of the storage capacity and the topographic index, $p_{w\kappa}(w,\kappa)$, i.e.,

$$p_w(w)=\int_{\kappa_{min}}^{\kappa_{max}}\delta\left(w-w_{max}\frac{\kappa_{max}-\kappa}{\kappa_{max}-\kappa_{min}}\right)p_\kappa(\kappa)d\kappa, \qquad (B3)$$

where $p_\kappa(\kappa)$ is the PDF of the topographic index and the conditional PDF $p_{w|\kappa}(w|\kappa)$ is a point mass of probability represented by a Dirac delta function $\delta(\cdot)$, which states that, with a probability of 1, the storage capacity, w, is equal to the r.h.s. of equation (B2). The topographic index distribution, $p_\kappa(\kappa)$, has been represented by a three parameter Gamma PDF [*Sivapalan et al.*, 1987, 1990; *Wolock et al.*, 1990; *Franchini et al.*, 1996] and an exponential function [*Niu et al.*, 2005]. For simplicity, we assume that $p_\kappa(\kappa)$ may be represented by an exponential PDF shifted by κ_{min} and truncated at κ_{max}, i.e.,

$$p_\kappa(\kappa)=C_1\frac{1}{\kappa_s}e^{-\frac{1}{\kappa_s}(\kappa-\kappa_{min})}, \qquad (B4)$$

where $\kappa_{min}\le\kappa<\kappa_{max}$, κ_s is the scale parameter, and C_1 is the normalization constant (see Table 4). The exponential CDF of equation (B4) well represents the larger topographic index values (e.g., Figures 7a and 7b) that correspond to the smaller values of w that produce the majority of the runoff according to the TOPMODEL runoff concept (see equation (B2)). For Davidson river case study, the parameters of equation (B4) are found by a nonlinear least squares fit of the corresponding cumulative distribution function (CDF) $C_1-C_1\exp\left(\frac{-\kappa+\kappa_{min}}{\kappa_s}\right)$ to the data of the cumulative distribution of the topographic index (see Table 3).

Appendix C: Practical Details

C1. Coding of the Gamma Function
While coding the Gamma function of equation (7), note that the lower incomplete gamma function may be written differently in common computer programs: in Matlab $\Gamma(a,z)=$ gammainc(z,a,'upper')*gamma(a) in
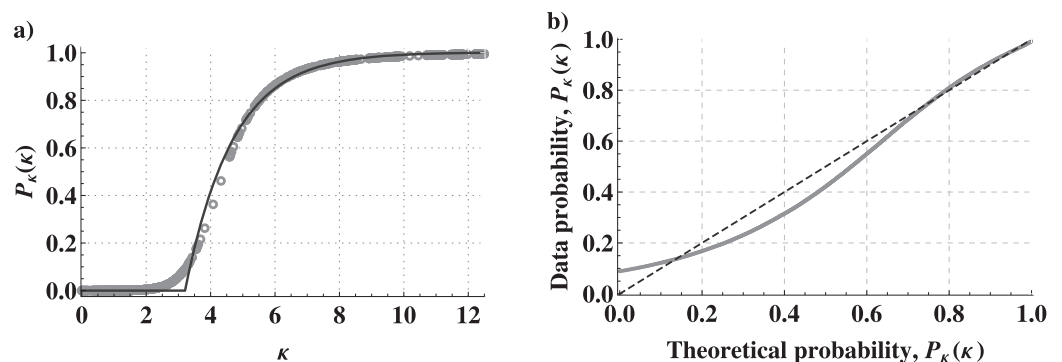

Figure 7. For the Davidson river watershed, comparison of (a) the empirical CDF of the topographic index (gray circles) with the theoretical CDF for the exponential PDF of equation (B4) (black line). Note the high agreement of the empirical and theoretical topographic index distributions for (b) larger probabilities that correspond to larger topographic index values with smaller storage capacities that are more likely to produce runoff.

Mathematica $\Gamma(a,z)=$ Gamma[a, z], while in Excel $\Gamma(a,z)=$ EXP(GAMMALN(a)) *(1-GAMMA.DIST(z,a,1, TRUE)), where in all cases the Gamma function, $\Gamma(a)$, results when $z=0$.

C2. Runoff PDFs and Averages for Exponentially Distributed Rainfall

We now present the prethreshold and threshold-excess runoff PDFs based on the exponential rainfall PDF of equation (6) and the soil moisture deficit and storage capacity PDF of equation (4) (see Table 2). Following equation (A6), the VICx/PDMx prethreshold runoff PDF is

$$p_{Q_p}(Q)=(1-\beta)\delta(Q)+\frac{\beta^2 e^{-Q\frac{\beta}{\bar{R}P_I}}}{(1-F_t(\bar{S},\bar{R}))\bar{R}P_I}\left(M(\bar{S})-\frac{Q\beta(1-P_I)}{P_I w_{\max}}\right)^{\frac{1}{\xi}},$$ (C1)

while for TOPMODELx the prethreshold runoff PDF is

$$p_{Q_p}(Q)=(1-\beta)\delta(Q)+\frac{\beta^2 e^{-Q\frac{\beta}{\bar{R}P_I}}C_1}{(1-F_t(\bar{S},\bar{R}))\bar{R}P_I}\left(1-e^{Q\frac{\beta(1-P_I)\xi}{P_I w_{\max}}}N(\bar{S})\right),$$ (C2)

where $0 \leq Q < L(\bar{S})$. For the limiting case of $\beta=0$, $p_{Q_p}(Q)=\delta(Q)$, which indicates that there is a discrete probability of zero runoff over the (prethreshold) unsaturated area, $1-F_t(\bar{S},\bar{R})$ (see Table 4).

For VICx/PDMx the threshold-excess runoff PDF found from equation (A7) is

$$p_{Q_t}(Q)=\frac{e^{-\frac{Q}{\bar{R}}}}{F_t(\bar{S},\bar{R})\bar{R}}\left((1-\beta)F_t(\bar{S},\bar{R})+\beta F_t\left(\bar{S},\bar{R}\frac{\beta}{\beta-P_I}\right)\right.$$
$$\left.-\Theta(L(\bar{S})-Q)\frac{\beta}{\xi}e^{-\frac{w_{\max}M(\bar{S})}{\bar{R}C_2}}\left(\frac{-w_{\max}}{\bar{R}C_2}\right)^{-\frac{1}{\xi}}\left(\Gamma\left(\frac{1}{\xi}\right)-\Gamma\left(\frac{1}{\xi},\frac{Q(\beta-P_I)}{\bar{R}P_I}-\frac{w_{\max}M(\bar{S})}{C_2\bar{R}}\right)\right)\right),$$ (C3)

while for TOPMODELx the threshold-excess runoff PDF is

$$p_{Q_t}(Q_t)=\frac{e^{-\frac{Q}{\bar{R}}}}{F_t(\bar{S},\bar{R})\bar{R}}\left((1-\beta)F_t(\bar{S},\bar{R})+\beta F_t\left(\bar{S},\bar{R}\frac{\beta}{\beta-P_I}\right)\right.$$
$$\left.-\Theta(L(\bar{S})-Q)\frac{\beta\bar{R}C_2 C_1\xi}{\bar{R}C_2\xi-w_{\max}}\left(N(\bar{S})^{\frac{w_{\max}}{\bar{R}C_2\xi}}-e^{Q\left(\frac{\beta(1-P_I)\xi}{P_I w_{\max}}-\frac{\beta-P_I}{\bar{R}P_I}\right)}N(\bar{S})\right)\right),$$ (C4)

where $\Theta(\cdot)$ is the Heaviside step function, and $F_t(\cdot,\cdot)$ is given by equations (7) and (8). For the limiting case of $\beta=0$, we recover equation (9) from equation (A5) with either equations (C1) and (C3) or equations (C2) and (C4). (see Table 4).

For VICx/PDMx, the average prethreshold runoff derived from the equation (C1) PDF is

$$\bar{Q}_p=\frac{\bar{R}P_I}{1-F_t(\bar{S},\bar{R})}\left(\frac{1+\xi}{\xi}(1-F_t(\bar{S},\bar{R}))-\frac{w_{\max}M(\bar{S})}{\bar{R}(1-P_I)}(F_t(\bar{S},\bar{R})-F(\bar{S}))\right),$$ (C5)

and the average threshold-excess runoff derived from the equation (C3) PDF is

$$\bar{Q}_t=\frac{\bar{R}}{F_t(\bar{S},\bar{R})}\left(F_t(\bar{S},\bar{R})-(1-F_t(\bar{S},\bar{R}))\frac{P_I}{\xi}+\frac{P_I w_{\max}M(\bar{S})}{\bar{R}(1-P_I)}(F_t(\bar{S},\bar{R})-F(\bar{S}))\right).$$ (C6)

For TOPMODELx, the average prethreshold runoff based on the equation (C2) PDF is

$$\bar{Q}_p=\frac{\bar{R}P_I}{1-F_t(\bar{S},\bar{R})}\left(1-F(\bar{S})-\frac{C_1\xi(w_{\max}-P_w^{-1}[F(\bar{S})])}{\bar{R}(1-P_I)\xi-w_{\max}}N(\bar{S})^{\frac{w_{\max}}{\bar{R}(1-P_I)\xi}}-(F_t(\bar{S},\bar{R})-F(\bar{S}))\frac{\bar{R}(1-P_I)\xi-2w_{\max}}{\bar{R}(1-P_I)\xi-w_{\max}}\right),$$ (C7)

while based on the equation (C4) PDF, the average threshold-excess runoff is

$$\bar{Q}_t=\frac{\bar{R}}{F_t(\bar{S},\bar{R})}\left(F(\bar{S})+\frac{P_I C_1\xi(w_{\max}-P_w^{-1}[F(\bar{S})])}{\bar{R}(1-P_I)\xi-w_{\max}}N(\bar{S})^{\frac{w_{\max}}{\bar{R}(1-P_I)\xi}}+(F_t(\bar{S},\bar{R})-F(\bar{S}))\frac{\bar{R}(1-P_I)\xi-(1+P_I)w_{\max}}{\bar{R}(1-P_I)\xi-w_{\max}}\right).$$ (C8)

For both VICx/PDMx and TOPMODELx, the average runoff, $\bar{Q}$, is the weighted sum of the prethreshold and threshold-excess runoff averages (see equation (A8)).

References

Arnell, N. (2014), *Hydrology and Global Environmental Change, Understanding Global Environ. Change*, Taylor and Francis, N. Y.

Au, C., and J. Tam (1999), Transforming variables using the Dirac generalized function, *Am. Stat.*, *53*(3), 270–272.

Bartlett, M. S., E. Daly, J. J. McDonnell, A. J. Parolari, and A. Porporato (2015), Stochastic rainfall-runoff model with explicit soil moisture dynamics, *Proc. R. Soc. A*, *471*(2183), 20150389.

Bartlett, M. S., A. J. Parolari, J. J. McDonnell, and A. Porporato (2016), Beyond the SCS-CN method: Framework for lumped rainfall-runoff response, *Water Resour. Res.*, *52*, 4608–4627, doi:10.1002/2015WR018439.

Bendat, J. S., and A. G. Piersol (2011), *Random Data: Analysis and Measurement Procedures*, vol. 729, John Wiley, Hoboken, N. J.

Beven, K. (2006), A manifesto for the equifinality thesis, *J. Hydrol.*, *320*(1), 18–36.

Beven, K. (2012), *Rainfall-Runoff Modelling: The Primer*, John Wiley, Hoboken, N. J.

Beven, K., and M. Kirkby (1979), A physically based, variable contributing area model of basin hydrology/un modèle à base physique de zone d'appel variable de l'hydrologie du bassin versant, *Hydrol. Sci. J.*, *24*(1), 43–69.

Carlston, C. W. (1963), *Drainage Density and Streamflow*, U.S. Govt. Print. Off., Washington, D. C.

Chapman, D. V. (Ed.) (1996), *Water Quality Assessments: A Guide to the Use of Biota, Sediments and Water in Environmental Monitoring*, E&FN Spon., Cambridge, U. K.

Chen, J., and Y. Wu (2012), Advancing representation of hydrologic processes in the soil and water assessment tool (SWAT) through integration of the topographic model (TOPMODEL) features, *J. Hydrol.*, *420*, 319–328.

Clark, M. P., A. G. Slater, D. E. Rupp, R. A. Woods, J. A. Vrugt, H. V. Gupta, T. Wagener, and L. E. Hay (2008), Framework for understanding structural errors (fuse): A modular framework to diagnose differences between hydrological models, *Water Resour. Res.*, *44*, W00B02, doi:10.1029/2007WR006735.

Descheemaeker, K., J. Nyssen, J. Poesen, D. Raes, M. Haile, B. Muys, and S. Deckers (2006), Runoff on slopes with restoring vegetation: A case study from the Tigray highlands, Ethiopia, *J. Hydrol.*, *331*(1), 219–241.

Dunne, T. (1983), Relation of field studies and modeling in the prediction of storm runoff, *J. Hydrol.*, *65*(1), 25–48.

Eckhardt, K. (2008), A comparison of baseflow indices, which were calculated with seven different baseflow separation methods, *J. Hydrol.*, *352*(1), 168–173.

Fenicia, F., D. Kavetski, and H. H. Savenije (2011), Elements of a flexible approach for conceptual hydrological modeling: 1. Motivation and theoretical development, *Water Resour. Res.*, *47*, W11510, doi:10.1029/2010WR010174.

Franchini, M., J. Wendling, C. Obled, and E. Todini (1996), Physical interpretation and sensitivity analysis of the TOPMODEL, *J. Hydrol.*, *175*(1), 293–338.

Freeze, R. A., and R. Harlan (1969), Blueprint for a physically-based, digitally-simulated hydrologic response model, *J. Hydrol.*, *9*(3), 237–258.

Habets, F., and G.-M. Saulnier (2001), Subgrid runoff parameterization, *Phys. Chem. Earth, Part B*, *26*(5), 455–459.

Hewlett, J. D., and A. R. Hibbert (1967), Factors affecting the response of small watersheds to precipitation in humid areas, in *Forest Hydrology*, edited by W. E. Sopper and H. W. Lull, pp. 275–290, Pergamon, N. Y.

Kavetski, D., G. Kuczera, and S. W. Franks (2003), Semidistributed hydrological modeling: A "saturation path" perspective on TOPMODEL and VIC, *Water Resour. Res.*, *39*(9), 1246, doi:10.1029/2003WR002122.

Liang, X., D. P. Lettenmaier, E. F. Wood, and S. J. Burges (1994), A simple hydrologically based model of land surface water and energy fluxes for general circulation models, *J. Geophys. Res.*, *99*(D7), 14,415–14,428.

Liang, X., D. P. Lettenmaier, E. F. Wood, and S. Burges (1996), One-dimensional statistical dynamic representation of subgrid spatial variability of precipitation in the two-layer variable infiltration capacity model, *J. Geophys. Res.*, *101*(21), 403–421.

McDonnell, J., et al. (2007), Moving beyond heterogeneity and process complexity: A new vision for watershed hydrology, *Water Resour. Res.*, *43*, W07301, doi:10.1029/2006WR005467.

McDonnell, J. J. (2013), Are all runoff processes the same?, *Hydrol. Processes*, *27*(26), 4103–4111.

Moore, R. (1985), The probability-distributed principle and runoff production at point and basin scales, *Hydrol. Sci. J.*, *30*(2), 273–297.

Moore, R. (2007), The PDM rainfall-runoff model, *Hydrol. Earth Syst. Sci.*, *11*(1), 483–499.

Moore, R., and R. Clarke (1981), A distribution function approach to rainfall runoff modeling, *Water Resour. Res.*, *17*(5), 1367–1382.

Niu, G.-Y., Z.-L. Yang, R. E. Dickinson, and L. E. Gulden (2005), A simple TOPMODEL-based runoff parameterization (SIMTOP) for use in global climate models, *J. Geophys. Res.*, *110*, D21106, doi:10.1029/2005JD006111.

Noto, L. V. (2013), Exploiting the topographic information in a PDM-based conceptual hydrological model, *J. Hydrol. Eng.*, *19*(6), 1173–1185.

Olver, F. W. J., D. W. Lozier, R. F. Boisvert, and C. W. Clark (Eds.) (2010), *NIST Handbook of Mathematical Functions*, Cambridge Univ. Press, N. Y.

Ponce, V. M., and R. H. Hawkins (1996), Runoff curve number: Has it reached maturity?, *J. Hydrol. Eng.*, *1*(1), 11–19.

Rodríguez-Iturbe, I., and A. Porporato (2004), *Ecohydrology of Water-Controlled Ecosystems: Soil Moisture and Plant Dynamics*, Cambridge Univ. Press, Cambridge, U. K.

Saleh, A., J. Arnold, P. W. A. Gassman, L. Hauck, W. Rosenthal, J. Williams, and A. McFarland (2000), Application of swat for the upper north Bosque river watershed, *Trans. ASAE*, *43*(5), 1077–1087.

Schaake, J. C., V. I. Koren, Q.-Y. Duan, K. Mitchell, and F. Chen (1996), Simple water balance model for estimating runoff at different spatial and temporal scales, *J. Geophys. Res.*, *101*(D3), 7461–7475.

Semenova, O., and K. Beven (2015), Barriers to progress in distributed hydrological modelling, *Hydrol. Processes*, *29*(8), 2074–2078.

Shuttleworth, W. J. (1988), Macrohydrology—The new challenge for process hydrology, *J. Hydrol.*, *100*(1), 31–56.

Sivapalan, M., K. Beven, and E. F. Wood (1987), On hydrologic similarity: 2. A scaled model of storm runoff production, *Water Resour. Res.*, *23*(12), 2266–2278.

Sivapalan, M., E. F. Wood, and K. J. Beven (1990), On hydrologic similarity: 3. A dimensionless flood frequency model using a generalized geomorphologic unit hydrograph and partial area runoff generation, *Water Resour. Res.*, *26*(1), 43–58.

Sivapalan, M., R. A. Woods, and J. D. Kalma (1997), Variable bucket representation of TOPMODEL and investigation of the effects of rainfall heterogeneity, *Hydrol. Processes*, *11*(9), 1307–1330.

Sloto, R. A., and M. Y. Crouse (1996), *HYSEP: A Computer Program for Streamflow Hydrograph Separation and Analysis*, U.S. Dep. of the Inter., U.S. Geol. Surv., Washington, D. C.

Tang, Q., T. Oki, S. Kanae, and H. Hu (2007), The influence of precipitation variability and partial irrigation within grid cells on a hydrological simulation, *J. Hydrometeorol.*, *8*(3), 499–512.

Tarboton, D. G., and I. N. Mohammed (2013), *Taudem 5.1 Quick Start Guide to Using the TauDEM ArcGIS Toolbox*, Utah State University, Logan, Utah. [Available at http://hydrology.usu.edu/taudem/taudem5/index.html.]

Thomas, G., and A. Henderson-Sellers (1991), An evaluation of proposed representations of subgrid hydrologic processes in climate models, *J. Clim.*, *4*(9), 898–910.

Tromp-van Meerveld, H., and J. McDonnell (2006a), Threshold relations in subsurface stormflow: 1. A 147-storm analysis of the panola hillslope, *Water Resour. Res.*, *42*, W02410, doi:10.1029/2004WR003778.

Tromp-van Meerveld, H., and J. McDonnell (2006b), Threshold relations in subsurface stormflow: 2. The fill and spill hypothesis, *Water Resour. Res.*, *42*, W02411, doi:10.1029/2004WR003800.

USDA National Resources Conservation Service (2004), *National Engineering Handbook: Part 630–Hydrology*, Washington, D. C.

Warrach, K., M. Stieglitz, H.-T. Mengelkamp, and E. Raschke (2002), Advantages of a topographically controlled runoff simulation in a soil-vegetation-atmosphere transfer model, *J. Hydrometeorol.*, *3*(2), 131–148.

Wine, M. L., C. B. Zou, J. A. Bradford, and S. A. Gunter (2012), Runoff and sediment responses to grazing native and introduced species on highly erodible Southern Great Plains soil, *J. Hydrol.*, *450*, 336–341.

Wolock, D., G. Hornberger, and T. Musgrove (1990), Topographic effects on flow path and surface water chemistry of the Llyn Brianne catchments in Wales, *J. Hydrol.*, *115*(1–4), 243–259.

Wood, E. F., D. P. Lettenmaier, and V. G. Zartarian (1992), A land-surface hydrology parameterization with subgrid variability for general circulation models, *J. Geophys. Res.*, *97*(D3), 2717–2728.

Yu, B. (1998), Theoretical justification of SCS method for runoff estimation, *J. Irrig. Drain. Eng.*, *124*(6), 306–310.